Regenerative Therapy 9 (2018) 71–78

Contents lists available at ScienceDirect

Regenerative Therapy

journal homepage: http://www.elsevier.com/locate/reth

Original Article

Epigenetic-scale comparison of human iPSCs generated by retrovirus, Sendai virus or episomal vectors

Koichiro Nishino [a, b], Yoshikazu Arai [a], Ken Takasawa [a], Masashi Toyoda [c], Mayu Yamazaki-Inoue [d], Tohru Sugawara [d], Hidenori Akutsu [d], Ken Nishimura [e], Manami Ohtaka [f], Mahito Nakanishi [g], Akihiro Umezawa [d, *]

[a] Laboratory of Veterinary Biochemistry and Molecular Biology, Graduate School of Medicine and Veterinary Medicine/Faculty of Agriculture, University of Miyazaki, Miyazaki, Japan
[b] Center for Animal Disease Control, University of Miyazaki, Miyazaki, Japan
[c] Research Team for Geriatric Medicine, Tokyo Metropolitan Institute of Gerontology, Tokyo, Japan
[d] Department of Reproductive Biology, Center for Regenerative Medicine, National Research Institute for Child Health and Development, Tokyo, Japan
[e] Laboratory of Gene Regulation, Faculty of Medicine, University of Tsukuba, Ibaraki, Japan
[f] TOKIWA-Bio, Inc., Ibaraki, Japan
[g] Biotechnology Research Institute for Drug Discovery, National Institute of Advanced Industrial Science and Technology (AIST), Ibaraki, Japan

ARTICLE INFO

Article history:
Received 12 July 2018
Received in revised form
9 August 2018
Accepted 9 August 2018

Keywords:
Human iPSCs
Human ESCs
DNA methylation
Aberrant methylation

ABSTRACT

Human induced pluripotent stem cells (iPSCs) are established by introducing several reprogramming factors, such as *OCT3/4, SOX2, KLF4, c-MYC*. Because of their pluripotency and immortality, iPSCs are considered to be a powerful tool for regenerative medicine. To date, iPSCs have been established all over the world by various gene delivery methods. All methods induced high-quality iPSCs, but epigenetic analysis of abnormalities derived from differences in the gene delivery methods has not yet been performed. Here, we generated genetically matched human iPSCs from menstrual blood cells by using three kinds of vectors, i.e., retrovirus, Sendai virus, and episomal vectors, and compared genome-wide DNA methylation profiles among them. Although comparison of aberrant methylation revealed that iPSCs generated by Sendai virus vector have lowest number of aberrant methylation sites among the three vectors, the iPSCs generated by non-integrating methods did not show vector-specific aberrant methylation. However, the differences between the iPSC lines were determined to be the number of random aberrant hypermethylated regions compared with embryonic stem cells. These random aberrant hypermethylations might be a cause of the differences in the properties of each of the iPSC lines.

1. Introduction

Human induced pluripotent stem cells (iPSCs) are powerful resources for disease modeling, drug discovery, and regenerative medicine because of their potential for pluripotency, ability to self-renew indefinitely, avoidance of rejection of their derivatives by the immune system and for ethical issues [1]. Studies of reprogramming mechanisms and characterization of iPSCs are imperative to ensure the safety of their derivatives in regenerative medicine [2]. Epigenetic reprogramming is an essential event during transformation from somatic cells to iPSCs. DNA methylation is an important epigenetic modification and has a critical role in many aspects of normal development and disease [3–5]. Expression of *OCT3/4* and *NANOG* genes, known as reprogramming factors, are induced in restricted tissues with an inverse correlation of DNA methylation during development [6,7]. Transient ectopic expression of defined reprogramming factors forces genome-wide epigenetic exchange and transforms somatic cells to iPSCs [8–12]. After reprogramming, epigenetic profiles of the human iPSCs can be clearly discriminated from the parent somatic cells and are similar to human embryonic stem cells (ESCs), though there is a small fraction of differentially methylated regions [11–15]. In addition, the degree of global DNA methylation in human pluripotent stem

* Corresponding author. Fax: +81 3 5494 7048.
E-mail address: umezawa@1985.jukuin.keio.ac.jp (A. Umezawa).
Peer review under responsibility of the Japanese Society for Regenerative Medicine.

https://doi.org/10.1016/j.reth.2018.08.002

cells, ESCs and iPSCs, is higher when compared to somatic cells [11,12]. This global hypermethylation of human pluripotent stem cells is a feature shared with primed murine epiblast stem cells, although mouse ESCs, that are naïve state stem cells, have global hypomethylation corresponding to early embryonic cells [16–21].

Human iPSCs have been established by various gene delivery methods. After the first report of iPSC generation by using retrovirus vectors [8], lentivirus vectors [22], Sendai virus vectors [23,24], PiggyBac vectors [10], plasmid vectors [25], episomal vectors [26], protein transfer [27,28], mRNA transfer [29], and miRNA transfer [30] have been reported as methods for iPSC generation. All methods induced high-quality iPSCs, but epigenetic abnormalities associated with the specific gene delivery method have not been well analyzed. In this study, we generated human iPSCs derived from menstrual blood cells with three kinds of vectors, i.e., retrovirus, Sendai virus, and episomal vectors, and evaluated them for the scale of genome-wide DNA methylation.

2. Results

2.1. Comparison of DNA methylation level in pluripotent stem cells and somatic cells

We generated genetically matched human iPSCs from menstrual blood cells (Edom22) in our laboratory by retrovirus vector infection [12], episomal vector transfection or Sendai viral SeVdp-iPS vector infection (designated as Retro-, Episomal-, and Sendai-iPSCs, respectively) (Fig. 1A and B, Supplemental Figs. 1 and 2). To investigate the differences in DNA methylation between iPSCs generated with the three kinds of vectors, we obtained DNA methylation profiles from ESCs, iPSCs including Retro-iPSCs, Sendai-iPSCs, and Episomal-iPSCs, and parent somatic cells, using Illumina's Infinium HumanMethylation450K BeadChip. Methylation levels are represented as β-values, which range from "0", for completely unmethylated, to "1", for completely methylated. Additional data sets from 5 ESCs were obtained from the GEO database [31]. We completely analyzed global DNA methylation of 49 samples (Supplemental Table 1), all with XX karyotypes. All iPSC lines in this study were derived from the same parental somatic cell, Edom22. The promoter regions of pluripotency-associated genes such as *POU5F1*, *NANOG*, *SALL4*, *PTPN6*, *RAB25*, *EPHA1*, *TDGF1* and *LEFTY1* showed low levels of methylation, whereas the promoter regions of somatic cell-associated genes such as *EMILIN1*, *LYST*, *RIN2* and *SP100* were highly methylated in all pluripotent cells (Fig. 1C). These results indicate that all iPSC lines were completely reprogrammed at the core genes, regardless of type of vector used. As assessed by unsupervised hierarchical cluster analysis (HCA) (Fig. 1D) and principal component analysis (PCA) (Fig. 1E) using each iPSC lines (passaged about 30 times), human iPSCs were clearly distinguishable from their parent cells and were similar to ESCs. Sendai-iPSCs appeared to be more similar to ESCs, but no clear difference among the three methods was defined.

2.2. Identification of differentially methylated regions

In further analysis, we defined a differentially methylated region (DMR) between ESCs and iPSCs as a CpG site whose delta-β-value score differed by at least 0.3 (Fig. 2A). We compared the DNA methylation states of each iPSC line with those of ESCs (the averaged value from 12 ESC lines). The number of DMRs between ESCs and each iPSC line (ES-iPS-DMRs) ranged from 448 to 1175 in Retro-iPSCs, from 101 to 168 in Sendai-iPSCs, and from 202 to 875 in Episomal-iPSCs. Sendai-iPSCs had lowest number of ES-iPS-DMRs among three kinds of vectors (Fig. 2B). The number of ES-iPS-DMRs in all 6 Sendai-iPSCs was under 168. In Episomal-iPSCs, 2 out of 3 lines showed 300 or fewer ES-iPS-DMRs. Although 1 out of 3 Retro-iPSC lines showed a relatively low number of ES-iPS-DMRs, the range of ES-iPS-DMRs number was wider. These results suggest that the number of ES-iPS-DMRs depended on each cell line rather than on the vectors used for iPSC generation. ES-iPS-DMRs can be categorized into two groups: hypermethylated and hypomethylated sites in iPSCs, as compared with ESCs. There was little difference in the number of hypomethylated ES-iPS-DMRs, especially between Sendai-iPSCs and Episomal-iPSCs (Fig. 2C). The difference between each iPSC line therefore appears to be dependent on the number of abnormal hypermethylated sites.

2.3. Correlation between expression of DNMT/TET genes and ES-iPS-DMRs

In order to investigate whether abnormal hypermethylation in iPSCs was caused by irregular expression of DNA methyltransferases (DNMTs) and/or Ten-eleven translocations (TETs) that induce demethylation, we examined expression level of *DNMT* and *TET* genes. All iPSC lines, regardless of type of vector, showed hyper expression of both *DNMT3B* and *TET1* genes compared to ESC (Fig. 2D and F). However, there was no correlation between the number of ES-iPS-DMRs and the expression levels of *DNMT3B* or *TET1* gene (Fig. 2E and G). Similarly, other *DNMTs* (*DNMT1*, *DNMT3A* and *DNMT3L*) and *TETs* (*TET2* and *TET3*) did not show correlation between the number of ES-iPS-DMRs and expression level (Supplemental Fig. 3).

2.4. Vector-specific ES-iPS-DMRs

We next aimed to detect vector-specific ES-iPS-DMR. We extracted 229 DMRs that overlapped in all 3 Retro-Edom-iPSC lines. The 44 and 76 DMRs also overlapped in all 6 Sendai-Edom-iPSC lines and in all 3 Episomal-Edom-iPSC lines, respectively (Fig. 3A). Approximately 80% of ES-iPS-DMR in each vector group was detected in only one or two lines, suggesting that most of the DMRs occurred randomly in the genome. Comparison of each the overlapping ES-iPS-DMR revealed that 167, 2, 13 ES-iPS-DMRs were detected as the Retro-, Sendai- and Episomal-iPSC-specific DMRs, respectively. Because these aberrant methylation sites at promoter region possibly affect gene expression, we further investigated ES-iPS-DMRs at promoters. While no ES-iPS-DMRs overlapped for all Sendai-iPSC lines, 44 and 5 ES-iPS-DMRs were common in all Retro- and Episomal-iPSC lines at the promoter regions, respectively (Fig. 3B). Details of vector-specific DMRs are summarized in Table 1 and Supplemental Table 2. Interestingly, 5 ES-iPS-DMRs in Episomal-iPSC lines appeared transiently. They were not DMRs at different passages and in different lines (Fig. 3C). In the Retro-iPSC line, 11 out of 44 ES-iPS-DMRs were also transient abnormal regions. These results indicated that Retro-iPSCs had a small subset of the vector-specific ES-iPS-DMRs, but iPSCs generated by non-integrating methods did not have the vector-specific ES-iPS-DMRs, especially those were located promoter regions.

2.5. Aberrant methylation in imprinted genes in pluripotent stem cells

We also compared DNA methylation of imprinted genes between somatic cells and iPSCs/ESCs, and identified 413 differentially methylated regions at promoter regions including 68 imprinted genes (Supplemental Table 3). These 68 genes comprised 69.4% of imprinted genes examined. Representative imprinted genes including *MEG3*, *H19*, *PEG3*, *IGFR2*, *PEG10* and *XIST* in ESCs and iPSCs showed aberrant methylation compared with parent somatic cells, independent of the vector type (Fig. 4). In addition, most of the aberrant methylation was not adapted during culture (Supplemental Fig. 4).

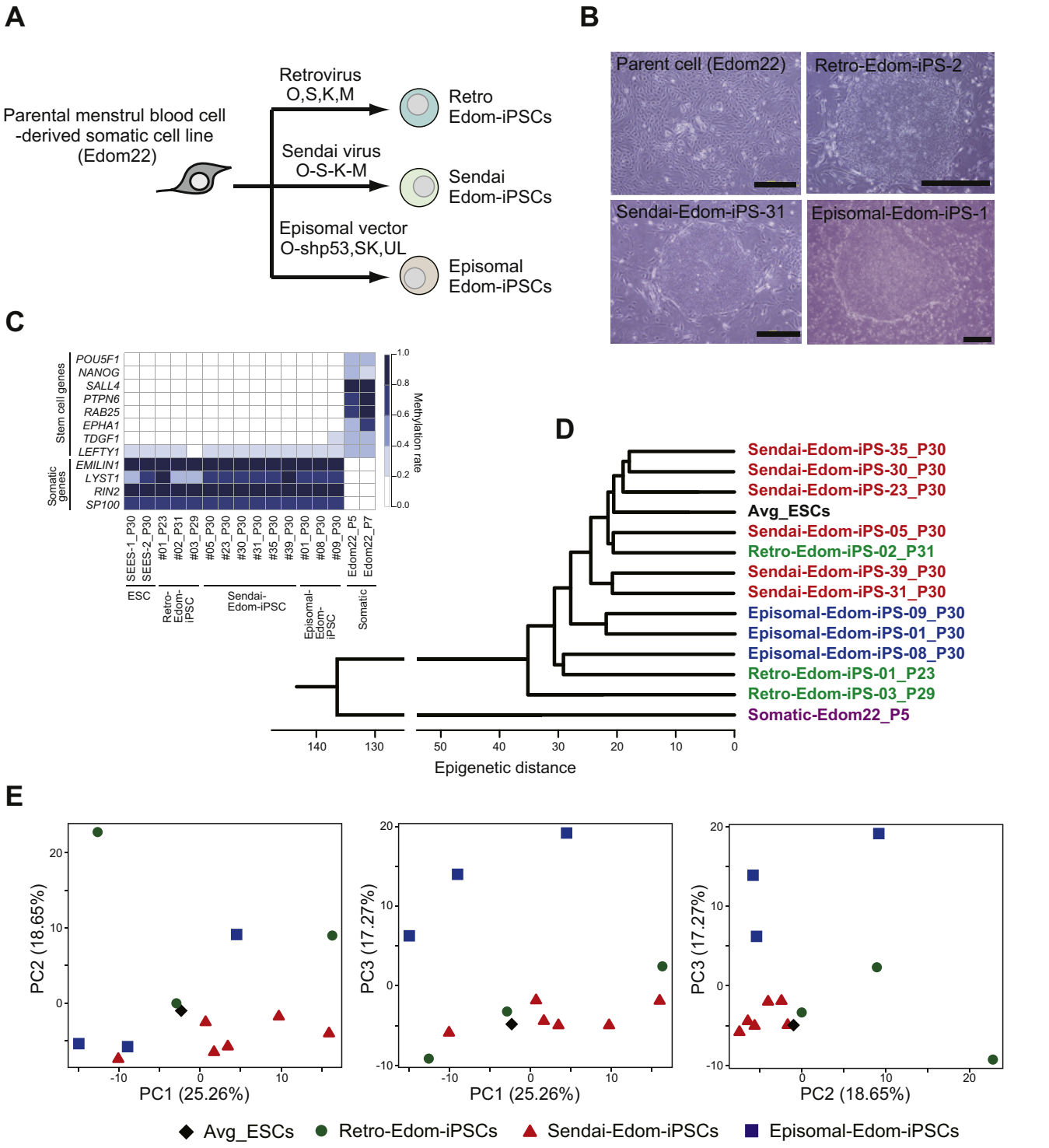

Fig. 1. Generation of genetically matched human iPSCs from the same parent somatic cells using three kinds of vectors. A, Schematic for generation of the genetically matched human iPSC lines. Human iPSCs were derived from the same parent somatic cell, Edom22 using retrovirus, Sendai virus and episomal vectors. B, Morphology of the parent somatic cells and iPSCs. Scale bars indicate 500 μm. C, Heatmap presenting DNA methylation levels at promoter regions of pluripotency-associated and somatic cell-associated genes. D, Unsupervised hierarchical clustering analysis (HCA) based on DNA methylation scores in the averaged ESCs (black), Retro-Edom-iPSCs (green), Sendai- Edom-iPSCs (red), Episomal-Edom-iPSCs (blue) and the parent somatic cell, Edom22 (purple). E, Principal component analysis (PCA) based on DNA methylation scores in the averaged ESCs (black diamond), Retro-iPSCs (green circles), Sendai-iPSCs (red triangles) and Episomal-iPSCs (blue squares).

3. Discussion

Choi et al. [32] reported that hiPSCs, which were generated by using a Sendai virus vector, were molecularly and functionally equivalent to genetically matched hESCs. Schlaeger et al. [33] also reported that there were no substantial method-specific differences in DNA methylation, marker expression levels or patterns, or developmental potential by comparing among Retro-, Lenti-, Sendai-, Episomal-, and mRNA-iPSCs. Our study bridges the gap between the two previous studies. In this study, we compared iPSC

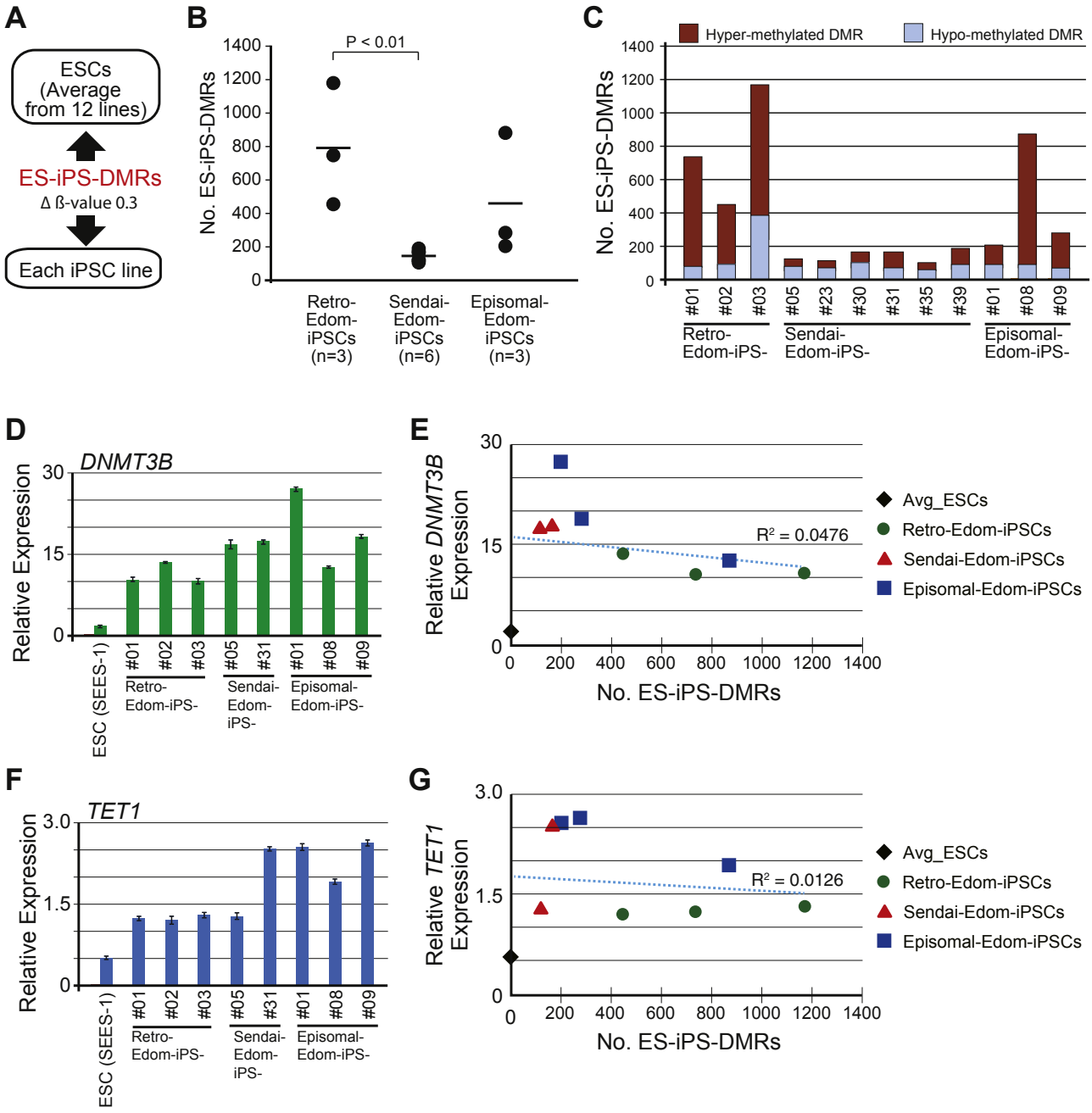

Fig. 2. Comparison of differentially methylated regions between ESCs and each iPSC line. A, Comparison of DNA methylation scores for each iPSC lines with that of the average for ESCs. The DMRs between the average for ESCs and iPSCs are designated as ES-iPS-DMRs. B, Comparison of the number of ES-iPS-DMRs in Retro-Edom-iPSCs (n = 3), Sendai- Edom-iPSCs (n = 6) and Episomal- Edom-iPSCs (n = 3). C, Proportion of the hyper and hypomethylated ES-iPS-DMRs in each iPSC lines. D, Quantitative RT-PCR for *hDNMT3B* in each PSC lines. E, Correlation between expression level of *hDNMT3B* and the number of ES-iPS-DMRs. The averaged ESCs, black diamond; Retro-iPSCs, green circles; Sendai-iPSCs, red triangles; Episomal-iPSCs, blue squares. F, Quantitative RT-PCR for *hTET1* in each PSC lines. G, Correlation between expression level of *hTET1* and the number of ES-iPS-DMRs. The averaged ESCs, black diamond; Retro-iPSCs, green circles; Sendai-iPSCs, red triangles; Episomal-iPSCs, blue squares.

lines derived from the same parental somatic cell line, menstrual blood-derived cells, using three types of vectors. Three types of menstrual blood cell-derived-iPSCs are preferable for comparison analysis to avoid any influence from different parental cells. Over 99% of CpG sites in all iPSC lines did not show differences in the methylation levels, compared with ESCs; therefore, iPSCs were almost identical to ESCs in epigenetics regardless of vector types used for iPSC generation. Our findings are consistent with the results of previous studies. However, when focusing the ES-iPS-DMRs of each iPSC line in details, we found that Sendai-iPSCs were more similar to ESCs than Retro- and Episomal-iPSCs at the epigenetic scale. Also, the ranges of the numbers of ES-iPS-DMRs among Retro-iPSC line was wider than those seen in Sendai- and Episomal-iPSCs. This wide variation might result from genome integration of transgenes. Among Episomal-iPSC lines, some lines as well as Sendai-iPSCs showed low numbers of DMRs. The differences between ESCs and iPSCs, especially Sendai- and Episomal-iPSCs, might be derived from characteristics of each of the iPSC lines, rather than type of vectors used for iPSC generation. The type of vector might influence the variety of line-specific properties. The

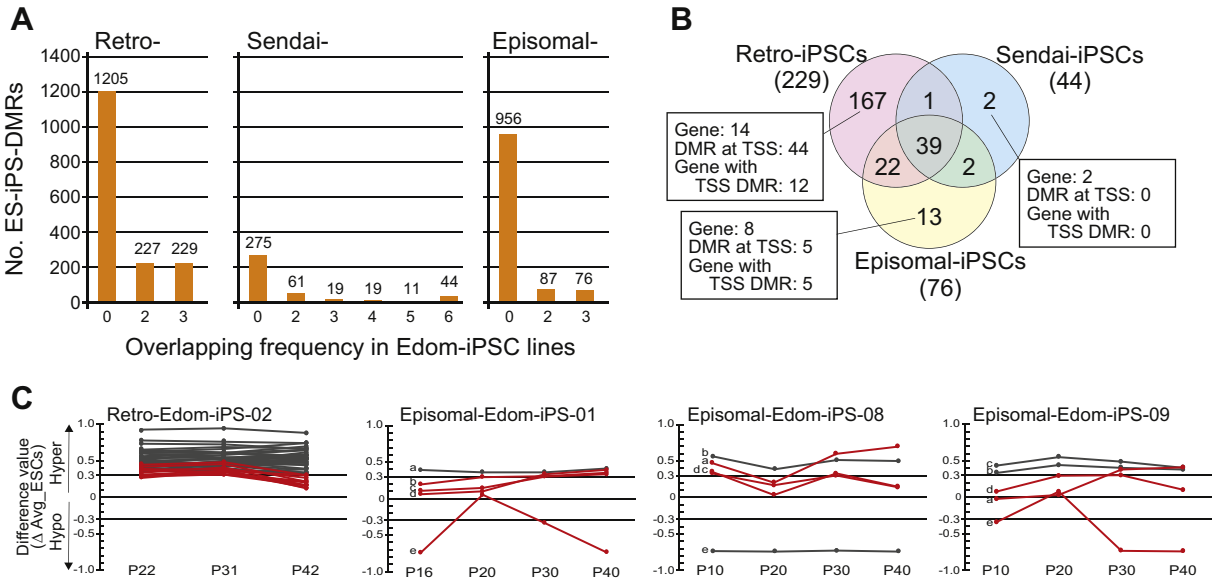

Fig. 3. Aberrant methylation in human iPSCs. A, The number of overlapping ES-iPS-DMRs in 3 Retro-Edom-iPSC lines, 6 Sendai-iPSC lines and 3 Episomal-iPSC lines. B, Venn diagram showing method-specific DMRs among three kinds of vectors. C, Effect of continuous cultivation on 44 and 5 ES-iPS-DMRs at TSS in Retro-iPSC line and in Episomal-iPSC lines, respectively. The difference values were estimated by subtracting the scores of the averaged ESCs from that of each passage sample. Each line shows a difference value of each probe during culture. Red lines represent transiently ES-iPS-DMRs, which are not DMR at different passage and in different line. a, *EPHA10* (probe ID: cg06163371), b, *WIPF2* (cg04977733), c, *FTH1* (cg25270670), d, *ZNF629* (cg05549854), e, *SLC19A1* (cg07658590).

Table 1
Details of the vector-specific DMRs.

Type of vector	Retrovirus	Sendai virus	Episomal	Common
a) No. DMR CpG	167	2	13	39
b) Hypermethylated DMR in a)	154	0	7	5
c) Hypomethylated DMR in a)	13	2	6	34
d) % Hypermethylated DMR (b/a)	92.22%	0.00%	53.85%	12.82%
e) No. DMR CpG on Gene locus in a)	121	2	10	28
f) % Gene locus (e/a)	72.46%	100.00%	76.92%	71.79%
g) Hypermethylated DMR in e)	117	0	7	2
h) Hypomethylated DMR in e)	4	2	3	26
i) % Hypermethylated DMR (f/e)	96.69%	0.00%	70.00%	7.14%
Relationship to canonical CpG Island[a]				
j) CpG island in e)	94	0	6	4
k) N_Shore in e)	8	1	1	4
l) N_Shelf in e)	1	0	0	2
m) S_Shore in e)	9	0	2	3
n) S_Shelf in e)	0	1	0	0
o) non-CpG island in e)	9	0	1	15
Gene region feature category[b]				
p) TSS1500 in e)	42	0	4	4
q) TSS200 in e)	24	0	2	4
r) 1stExon in e)	22	0	2	4
s) 5'UTR in e)	30	0	3	3
t) Body in e)	94	2	5	60
u) 3'UTR in e)	2	0	0	9
v) No, Gene in e)	14	2	8	41
W) No. probe in p) and q)	44	0	5	6
x) No. Gene with TSS-DMR (v and w)	12	0	5	6

[a] Relationship to canonical CpG Island: Shores, - 0–2 kb from CpG island; Shelves, - 2–4 kb from CpG island; N, upstream of CpG island; S, downstream of CpG island.
[b] Gene region feature category: Gene region feature category describing the CpG position, from UCSC. TSS200 = 0–200 bases upstream of the transcriptional start site (TSS). TSS1500 = 200–1500 bases upstream of the TSS. 5′UTR = Within the 5′ untranslated region, between the TSS and the ATG start site. Body = Between the ATG and stop codon; irrespective of the presence of introns, exons, TSS, or promoters. 3′UTR = Between the stop codon and poly A signal. This information on HumanMethylation450K was provided by Illumina Inc.

line-specific differences depended on the number of aberrant hypermethylated DMRs. There was no correlation between this aberrant hypermethylation and the expression levels of the *DNMT* or *TET* genes; therefore, this aberrant hypermethylation might be generated at the initial reprogramming step and maintained during culture. Approximately 80% of aberrant hypermethylated ES-iPS-

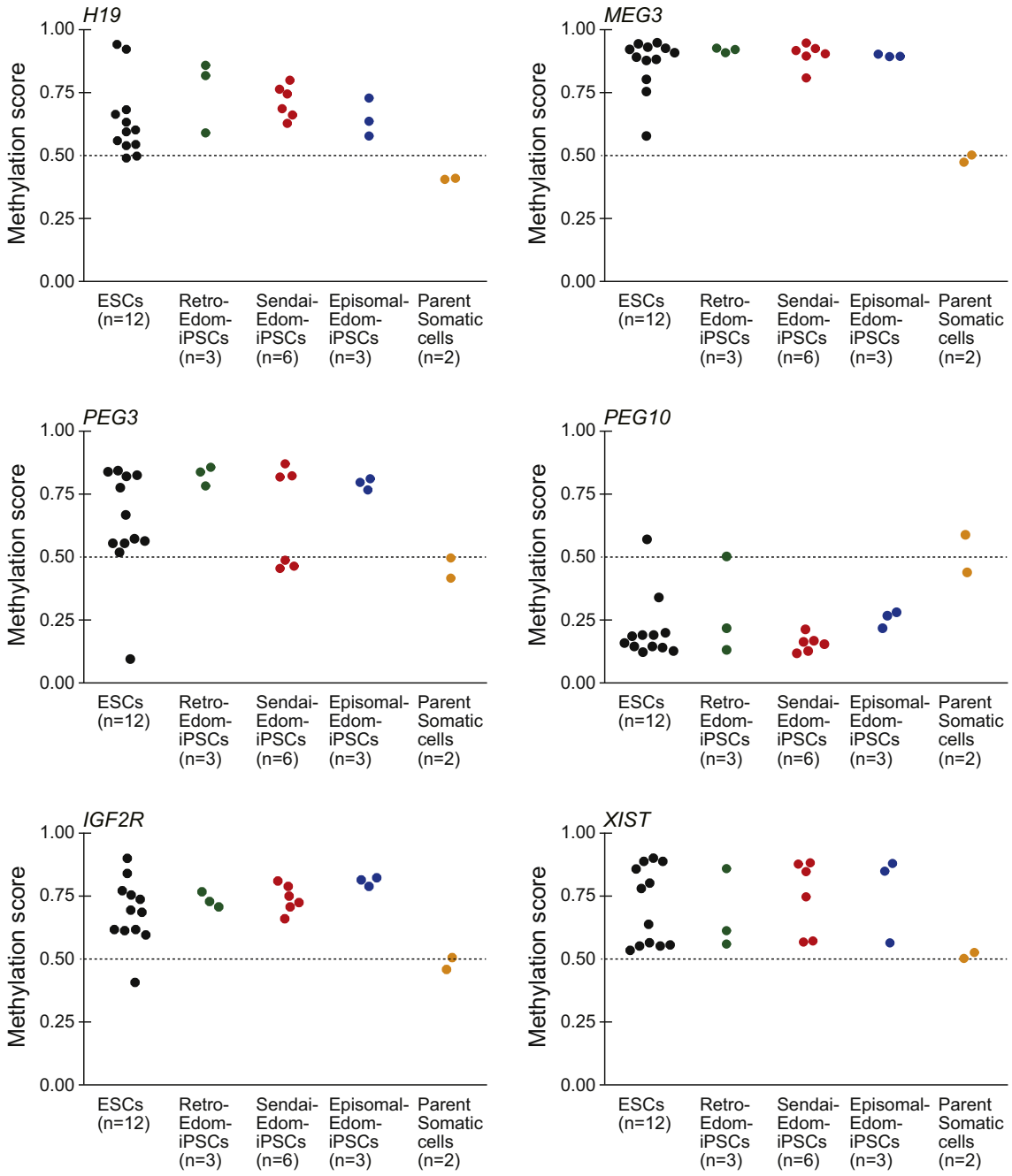

Fig. 4. Distribution of methylation scores at promoters of imprint genes and *XIST* gene. *H19*, *MEG3*, *PEG3*, *PEG10*, *IGF2R* and *XIST* genes are shown. ESCs (n = 12, black circles); Retro-Edom-iPSCs (n = 3, green circles); Sendai-Edom-iPSCs (n = 6, red circles); Episomal-Edom-iPSCs (n = 3, blue circles); parent somatic cells, Edom22 (n = 2, yellow circles). The probe IDs and probe positions of each gene were cg17985533, TSS200 for *H19*, cg09926418, TSS200 for *MEG3*, cg13960339, TSS200 for *PEG3*, cg27504782, TSS1500 for *PEG10*, cg10894318, TSS1500 for *IGF2R* and cg11717280, TSS200 for *XIST*. TSS200 and TSS1500 indicated the position of the probe; TSS200, 0–200 bases and TSS1500, 200–1500 bases upstream of the transcriptional start site (TSS).

DMR in each vector group was detected in only one or two lines and there were no vector-specific DMRs in non-integrating methods, suggesting that most of the DMRs occurred randomly in the genome. Therefore, this random hypermethylation might be a cause of the differences in the properties of each of the iPSC lines.

Aberrant methylation of some imprinted genes in ESCs and iPSCs have been reported by several groups [12,34,35]. In this study, we detected 68 imprinted genes that exhibited aberrant methylation, which comprised 69.4% of imprinted genes examined. These abnormalities have been widely detected in pluripotent stem cells. Most iPSC lines as well as ESCs, were abnormally hypermethylated at *MEG3*, *H19*, *PEG3*, *IGFR2* and *XIST*, regardless of the vector type. The aberrant methylation at imprinted gene and *XIST* gene promoters was maintained throughout continuous passage. The aberrant methylation of imprinted genes should therefore be monitored for validation of PSC quality.

In conclusion, we compared genetically matched iPSCs and revealed that there were no vector-specific aberrant methylated regions in iPSCs generated by non-integrating methods. The line-specific properties depended on the number of random aberrant

hypermethylated DMRs rather than type of vectors used for iPSC generation. The differences between the vectors might influence the variety of line-specific properties. It is noteworthy that epigenetic information can be useful to determine iPSC quality.

4. Materials and methods

4.1. Ethics statement

Human cells were collected with ethical approval of the Institutional Review Board of National Institute for Child Health and Development, Japan. Signed informed consent was obtained from donors, and the specimens were irreversibly de-identified. All experiments handling human cells and tissues were performed in line with the Tenets of the Declaration of Helsinki.

4.2. Human cell culture

Menstrual blood (Edom22) cells were independently established in our laboratory [36,37], and were maintained in the POWEREDBY10 medium (Glyco Technica Ltd., Sapporo, Japan). Human Retro-iPSCs were generated from Edom22 by retroviral vector pMXs, which encodes the cDNA for human *OCT3/4*, *SOX2*, *c-MYC*, and *KLF4*, via previously described procedures [8] with slight modifications [11,36,38,39]. Episomal-iPSCs were established from Edom22 by episomal vectors, pCXLE-hOCT3/4-shp53, pCXLE-hSK, and pCXLE-hUL, via procedures described [26]. Sendai-iPSCs were produced from Edom22 by Sendai viral vector SeVdp-iPS, which encodes the polycistronic cDNAs for mouse *Oct3/4*, *Sox2*, *c-Myc*, and *Klf4*, via procedures described [24]. These iPSCs clearly showed human ESC-like characters in terms of morphology; gene expression of stem cell markers; cell-surface antigens; growth (over than 20 passages); normal karyotypes; and teratoma formation (Supplemental Figs. 1 and 2). Non-integrating episomal vectors in the genome or erasing SeVdp vector RNA genome was also confirmed. Human ESCs, SEES, were generated in our laboratory [40]. Human iPSCs and ESCs were maintained on irradiated MEFs in iPSellon medium (Cardio Incorporated, Osaka, Japan) supplemented with 10 ng/ml recombinant human basic fibroblast growth factor (bFGF, Wako Pure Chemical Industries, Ltd., Osaka, Japan). ESC genomes [41,42] were kindly gifted from Drs. C. Cowan and T. Tenzan (Harvard Stem Cell Institute, Harvard University, Cambridge, MA).

4.3. DNA methylation analysis

DNA methylation analysis was performed using the Illumina infinium assay with the HumanMethylation450K BeadChip (Illumina Inc.). Genomic DNA was extracted from the cells using QIAamp DNA Mini Kit (Qiagen). One microgram of genomic DNA from each sample was bisulfite-converted using EZ DNA Methylation kit (Zymo Research), according to the manufacturer's recommendations. Bisulfite-converted genomic DNA was hybridized to the HumanMethylation450K BeadChip and the BeadChip was scanned on a BeadArray Reader (Illumina inc.), according to the manufacturer's instructions. Methylated and unmethylated signals were used to compute a β-value, which was a quantitative score of DNA methylation levels, ranging from “0”, for completely unmethylated, to “1”, for completely methylated. On the HumanMethylation450K BeadChip, oligonucleotides for 485,577 CpG sites covering more than 96% of Refseq and 95% of CpG islands were mounted. The probe with MAF (minor allele frequency of the overlapping variant) $\geq$ 5% [43] and CpG sites with $\geq$0.05 “Detection p value” (computed from the background based on negative controls) were eliminated from the data for further analysis, leaving 416,528 CpGs valid for use with the 49 samples tested. Average methylation was calculated from ESCs, in which 46,681 DMRs among each ESC line in each set were removed. In Fig. 1C, each iPSC line (at about the 30th passage) was used and the probes were follows; *POU5F1* (cg15948871, TSS1500), *NANOG* (cg25540142, TSS200), *SALL4* (cg25570495, TSS200), *PTPN6* (cg12690127, TSS200), *RAB25* (cg15896939, TSS200), *EPHA1* (cg02376703, TSS200), *TDGF1* (cg27371741, TSS200), *LEFTY1* (cg15604953, TSS1500), *EMILIN1* (cg19399165, TSS200), *LYST* (cg13677741, TSS1500), *RIN2* (cg17016000, TSS1500), *SP100* (cg23539753, TSS200). TSS200 and TSS1500 indicated the position of the probe; TSS200, 0−200 bases and TSS1500, 200−1500 bases upstream of the transcriptional start site (TSS).

4.4. Quantitative reverse transcription-PCR

Total RNA was extracted from samples by the conventional method using ISOGEN II (NIPPON GENE, Toyama, Japan). An aliquot of total RNA was reverse-transcribed using ReverTra Ace (TOYOBO, Japan) with random hexamer primers. The cDNA template was amplified using specific primers for *DNMT1, DNMT3A, DNMT3B, DNMT3L, TET1, TET2* and *TET3*. Expression of glyceraldehyde-3-phosphate dehydrogenase (*GAPDH*) was used as a control. Primers used in this study are summarized in Supplemental Table 4. Quantitative PCR was performed in at least triplicate for each sample on LightCycler®96 Real-Time PCR system (Roche) with Power SYBR Green PCR Master Mix (Life Technologies) using a standard protocol. Relative expression was calculated by the ddCT method using *GAPDH* as an internal standard.

4.5. Accession numbers

NCBI GEO: HumanMethylation450K BeadChip data in this study has been submitted under accession number GSE73938 and GSE116924. Additional data sets of 5 ESCs were obtained from GSE31848.

Author contributions

Conceived and designed the experiments: KoN AU. Performed the experiments: KoN KT MT MY-I. Analyzed the data: KoN. Contributed reagents/materials/analysis tools: KoN YA KT MT MY-I TS KeN MO MN HA. Wrote the paper: KoN AU.

Conflicts of interest

The authors declare that they have no conflict of interest.

Acknowledgments

We would like to express our sincere thanks to Drs. C. Cowan and T. Tenzan for HUESC lines, to Dr. H. Makino for establishing the Edom22 cells, to Ms. Y. Takahashi for bioinformatics analyses. This research was supported in part by AMED under Grant Number JP18bm0704003 to KoN, and by grants from the Ministry of Education, Culture, Sports, Science, and Technology (MEXT) of Japan; by Ministry of Health, Labor and Welfare (MHLW) Sciences research grant to AU.

Appendix A. Supplementary data

Supplementary data related to this article can be found at https://doi.org/10.1016/j.reth.2018.08.002.

References

[1] Park IH, Arora N, Huo H, Maherali N, Ahfeldt T, Shimamura A, et al. Disease-specific induced pluripotent stem cells. Cell 2008;134(5):877–86.
[2] Teshigawara R, Cho J, Kameda M, Tada T. Mechanism of human somatic reprogramming to iPS cell. Lab Invest 2017;97(10):1152–7.
[3] Li E. Chromatin modification and epigenetic reprogramming in mammalian development. Nat Rev Genet 2002;3(9):662–73.
[4] Reik W. Stability and flexibility of epigenetic gene regulation in mammalian development. Nature 2007;447(7143):425–32.
[5] Feng S, Jacobsen SE, Reik W. Epigenetic reprogramming in plant and animal development. Science 2010;330(6004):622–7.
[6] Hattori N, Nishino K, Ko YG, Hattori N, Ohgane J, Tanaka S, et al. Epigenetic control of mouse Oct-4 gene expression in embryonic stem cells and trophoblast stem cells. J Biol Chem 2004;279(17):17063–9.
[7] Hattori N, Imao Y, Nishino K, Hattori N, Ohgane J, Yagi S, et al. Epigenetic regulation of Nanog gene in embryonic stem and trophoblast stem cells. Gene Cell 2007;12(3):387–96.
[8] Takahashi K, Tanabe K, Ohnuki M, Narita M, Ichisaka T, Tomoda K, et al. Induction of pluripotent stem cells from adult human fibroblasts by defined factors. Cell 2007;131(5):861–72.
[9] Park IH, Zhao R, West JA, Yabuuchi A, Huo H, Ince TA, et al. Reprogramming of human somatic cells to pluripotency with defined factors. Nature 2008;451(7175):141–6.
[10] Woltjen K, Michael IP, Mohseni P, Desai R, Mileikovsky M, Hamalainen R, et al. piggyBac transposition reprograms fibroblasts to induced pluripotent stem cells. Nature 2009;458(7239):766–70.
[11] Nishino K, Toyoda M, Yamazaki-Inoue M, Makino H, Fukawatase Y, Chikazawa E, et al. Defining hypo-methylated regions of stem cell-specific promoters in human iPS cells derived from extra-embryonic amnions and lung fibroblasts. PLoS One 2010;5(9):e13017.
[12] Nishino K, Toyoda M, Yamazaki-Inoue M, Fukawatase Y, Chikazawa E, Sakaguchi H, et al. DNA methylation dynamics in human induced pluripotent stem cells over time. PLoS Genet 2011;7(5):e1002085.
[13] Lister R, Pelizzola M, Dowen RH, Hawkins RD, Hon G, Tonti-Filippini J, et al. Human DNA methylomes at base resolution show widespread epigenomic differences. Nature 2009;462(7271):315–22.
[14] Doi A, Park IH, Wen B, Murakami P, Aryee MJ, Irizarry R, et al. Differential methylation of tissue- and cancer-specific CpG island shores distinguishes human induced pluripotent stem cells, embryonic stem cells and fibroblasts. Nat Genet 2009;41(12):1350–3.
[15] Lister R, Pelizzola M, Kida YS, Hawkins RD, Nery JR, Hon G, et al. Hotspots of aberrant epigenomic reprogramming in human induced pluripotent stem cells. Nature 2011;471(7336):68–73.
[16] Nichols J, Smith A. Naive and primed pluripotent states. Cell Stem Cell 2009;4(6):487–92.
[17] Tesar PJ, Chenoweth JG, Brook FA, Davies TJ, Evans EP, Mack DL, et al. New cell lines from mouse epiblast share defining features with human embryonic stem cells. Nature 2007;448(7150):196–9.
[18] Habibi E, Brinkman AB, Arand J, Kroeze LI, Kerstens HH, Matarese F, et al. Whole-genome bisulfite sequencing of two distinct interconvertible DNA methylomes of mouse embryonic stem cells. Cell Stem Cell 2013;13(3):360–9.
[19] Ficz G, Hore TA, Santos F, Lee HJ, Dean W, Arand J, et al. FGF signaling inhibition in ESCs drives rapid genome-wide demethylation to the epigenetic ground state of pluripotency. Cell Stem Cell 2013;13(3):351–9.
[20] Leitch HG, McEwen KR, Turp A, Encheva V, Carroll T, Grabole N, et al. Naive pluripotency is associated with global DNA hypomethylation. Nat Struct Mol Biol 2013;20(3):311–6.
[21] Yagi M, Yamanaka S, Yamada Y. Epigenetic foundations of pluripotent stem cells that recapitulate in vivo pluripotency. Lab Invest 2017;97(10):1133–41.
[22] Shao L, Feng W, Sun Y, Bai H, Liu J, Currie C, et al. Generation of iPS cells using defined factors linked via the self-cleaving 2A sequences in a single open reading frame. Cell Res 2009;19(3):296–306.
[23] Fusaki N, Ban H, Nishiyama A, Saeki K, Hasegawa M. Efficient induction of transgene-free human pluripotent stem cells using a vector based on Sendai virus, an RNA virus that does not integrate into the host genome. Proc Jpn Acad Ser B 2009;85(8):348–62.
[24] Nishimura K, Sano M, Ohtaka M, Furuta B, Umemura Y, Nakajima Y, et al. Development of defective and persistent Sendai virus vector: a unique gene delivery/expression system ideal for cell reprogramming. J Biol Chem 2011;286(6):4760–71.
[25] Okita K, Nakagawa M, Hyenjong H, Ichisaka T, Yamanaka S. Generation of mouse induced pluripotent stem cells without viral vectors. Science 2008;322(5903):949–53.
[26] Okita K, Matsumura Y, Sato Y, Okada A, Morizane A, Okamoto S, et al. A more efficient method to generate integration-free human iPS cells. Nat Methods 2011;8(5):409–12.
[27] Zhou H, Wu S, Joo JY, Zhu S, Han DW, Lin T, et al. Generation of induced pluripotent stem cells using recombinant proteins. Cell Stem Cell 2009;4(5):381–4.
[28] Kim D, Kim CH, Moon JI, Chung YG, Chang MY, Han BS, et al. Generation of human induced pluripotent stem cells by direct delivery of reprogramming proteins. Cell Stem Cell 2009;4(6):472–6.
[29] Warren L, Manos PD, Ahfeldt T, Loh YH, Li H, Lau F, et al. Highly efficient reprogramming to pluripotency and directed differentiation of human cells with synthetic modified mRNA. Cell Stem Cell 2010;7(5):618–30.
[30] Anokye-Danso F, Trivedi CM, Juhr D, Gupta M, Cui Z, Tian Y, et al. Highly efficient miRNA-mediated reprogramming of mouse and human somatic cells to pluripotency. Cell Stem Cell 2011;8(4):376–88.
[31] Nazor KL, Altun G, Lynch C, Tran H, Harness JV, Slavin I, et al. Recurrent variations in DNA methylation in human pluripotent stem cells and their differentiated derivatives. Cell Stem Cell 2012;10(5):620–34.
[32] Choi J, Lee S, Mallard W, Clement K, Tagliazucchi GM, Lim H, et al. A comparison of genetically matched cell lines reveals the equivalence of human iPSCs and ESCs. Nat Biotechnol 2015;33(11):1173–81.
[33] Schlaeger TM, Daheron L, Brickler TR, Entwisle S, Chan K, Cianci A, et al. A comparison of non-integrating reprogramming methods. Nat Biotechnol 2015;33(1):58–63.
[34] Rugg-Gunn PJ, Ferguson-Smith AC, Pedersen RA. Epigenetic status of human embryonic stem cells. Nat Genet 2005;37(6):585–7.
[35] Rugg-Gunn PJ, Ferguson-Smith AC, Pedersen RA. Status of genomic imprinting in human embryonic stem cells as revealed by a large cohort of independently derived and maintained lines. Hum Mol Genet 2007;16(Spec No. 2):R243–51.
[36] Nagata S, Toyoda M, Yamaguchi S, Hirano K, Makino H, Nishino K, et al. Efficient reprogramming of human and mouse primary extra-embryonic cells to pluripotent stem cells. Gene Cell 2009;14(12):1395–404.
[37] Cui CH, Uyama T, Miyado K, Terai M, Kyo S, Kiyono T, et al. Menstrual blood-derived cells confer human dystrophin expression in the murine model of Duchenne muscular dystrophy via cell fusion and myogenic trans-differentiation. Mol Biol Cell 2007;18(5):1586–94.
[38] Makino H, Toyoda M, Matsumoto K, Saito H, Nishino K, Fukawatase Y, et al. Mesenchymal to embryonic incomplete transition of human cells by chimeric OCT4/3 (POU5F1) with physiological co-activator EWS. Exp Cell Res 2009;315(16):2727–40.
[39] Toyoda M, Yamazaki-Inoue M, Itakura Y, Kuno A, Ogawa T, Yamada M, et al. Lectin microarray analysis of pluripotent and multipotent stem cells. Gene Cell 2011;16(1):1–11.
[40] Akutsu H, Machida M, Kanzaki S, Sugawara T, Ohkura T, Nakamura N, et al. Xenogeneic-free defined conditions for derivation and expansion of human embryonic stem cells with mesenchymal stem cells. Regen Ther 2015;1:18–29.
[41] Cowan CA, Klimanskaya I, McMahon J, Atienza J, Witmyer J, Zucker JP, et al. Derivation of embryonic stem-cell lines from human blastocysts. N Engl J Med 2004;350(13):1353–6.
[42] Osafune K, Caron L, Borowiak M, Martinez RJ, Fitz-Gerald CS, Sato Y, et al. Marked differences in differentiation propensity among human embryonic stem cell lines. Nat Biotechnol 2008;26(3):313–5.
[43] Okamura K, Kawai T, Hata K, Nakabayashi K. Lists of HumanMethylation450 BeadChip probes with nucleotide-variant information obtained from the phase 3 data of the 1000 genomes project. Genom Data 2016;7:67–9.